

High-temperature internal friction and dynamic moduli in copper

Emmanuel C. David^{a,*}, Ian Jackson^a

^a Research School of Earth Sciences, Australian National University, Canberra, Australia



ARTICLE INFO

Keywords:

Internal friction
Fcc metals
High-temperature peak
Burgers rheology
Dislocation migration
Harper-Dorn creep

ABSTRACT

New measurements of dynamic shear and Young's moduli and their associated internal frictions were made with torsional and flexural forced-oscillation methods, respectively, on three polycrystalline specimens of pure copper. The tests spanned the 1–1000 s range of oscillation periods, at temperatures ranging from those of annealing close to the melting point (1050 °C) down to room temperature. A broad internal friction peak, found at temperatures around 700 °C (at 1 Hz) for samples annealed at 1050 °C, is superimposed on a monotonic relaxation background. Non-linear viscoelastic behaviour is observed above strains around 5×10^{-6} . The period- and temperature-dependence of both shear modulus and internal friction is adequately captured by an extended “background plus peak” Burgers model for viscoelastic rheology. Activation energies are found to be around 200 kJ mol^{-1} for both the high-temperature peak and monotonic damping background, consistent with common diffusional control of both the dissipation background and superimposed peak, plausibly involving stress-induced migration of dislocations. Complementary torsional microcreep tests at selected temperatures reveal that most of the inelastic strain is anelastic (viscous) for loading durations less (greater) than 1000 s. Such linear viscous deformation, observed at low stress in coarse-grained polycrystalline copper, involves much higher strain rates than expected from published rheology, plausibly attributable to the Harper-Dorn mechanism.

1. Introduction

Knowledge of internal friction in metals is essential for a wide range of engineering applications, as well as providing a tool to study internal structure and relaxation mechanisms. Among commonly engineered fcc metals, copper, like more widely studied aluminium, offers the possibility to investigate temperature-dependent viscoelastic relaxation up to melting point. Since the pioneering work of Kê [1,2], many experimental studies of damping in metals employed the torsional pendulum arrangement, embedded in a furnace, under controlled atmosphere (e.g., [3–9]). Whereas most early studies focused on the effect of temperature at the essentially fixed resonance frequency of a pendulum, forced oscillation methods allow for *mechanical spectroscopy* over a wide frequency band ($\sim 0.1 \text{ mHz}$ –10 Hz), culminating in the work of Gaboriaud et al. [10] and related coauthors. For a broad review of the relevant phenomenology, experimental techniques, and their applications see Nowick and Berry [11] and Schaller et al. [12].

Specimens of polycrystalline copper typically exhibit internal friction peak(s) superimposed on a damping background (e.g., [1,13–15,8,16]). Both the number of peaks present, and the conditions under which these peaks occur, have been the subject of a continuing debate (e.g., [17–19]). Kê [1] measured a low-temperature peak on a

pure aluminium polycrystal that was absent in single-crystal material. On pure copper, deMorton and Leak [20] and Roberts and Barrand [14] demonstrated that such a peak disappears after annealing at sufficiently high temperatures, while Williams and Leak [13] defined different categories of peaks associated with different relaxation processes. Internal friction has also been observed to be strongly sensitive to the maximal strain amplitude used in forced-oscillation tests [3,21], and to other experimental conditions such as the presence of impurities, or prior cold work.

Damping in polycrystalline fcc metals was initially attributed to grain-boundary sliding and migration by Kê [22], followed by similar interpretations invoking the viscous behaviour of grain boundaries [20,6]. In contrast, the substantial body of detailed work by Woignard, Rivière and collaborators, (e.g., [15,21]) seems to indicate that much of the damping originates from lattice dislocation-related processes, and that grain boundaries have only an indirect influence through interaction with dislocations. In fact, these authors observed a significant difference between values of internal friction measured on single and polycrystals only in background damping [23]. Their interpretation was supported by comparing peak activation and self-volume diffusion energies. However, some assessments of inter-granular relaxation *versus* intra-granular relaxation are more equivocal (Povolo and Molinas [17],

* Corresponding author at:

E-mail address: e.david@ucl.ac.uk (E.C. David).

¹ Present address: Department of Earth Sciences, University College London, London, United Kingdom.

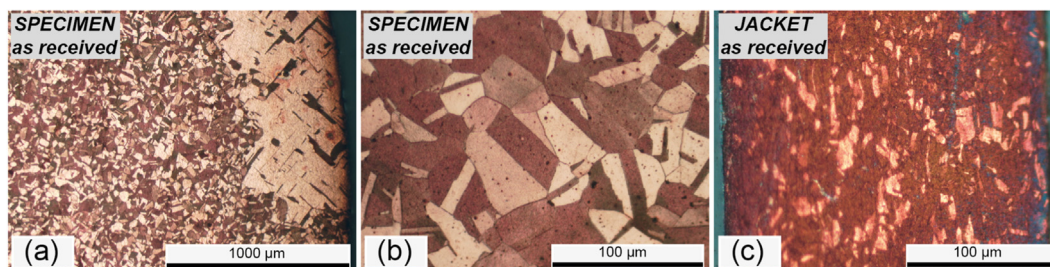


Fig. 1. Transverse sections of the starting copper specimen (a,b) and jacket (c). Sections were sawn, ground, polished and then etched with an aqueous solution containing 25 % HCl and 5 % $\text{Fe}(\text{NO}_3)_3$ to reveal grain structure under reflected light.

Benoit [18,24]). These authors emphasize strong evidence of grain-boundary involvement provided by grain-size sensitivity of anelastic relaxation in fine-grained materials, and the observation that relaxation scales with the number of grain boundaries that straddle the entire cross-section of a wire specimen with a “bamboo” structure.

However, there is not yet a published study that provides comprehensive measurements on polycrystalline copper, of internal friction and modulus in both torsion and in flexure, over wide ranges of both frequency and temperature approaching the melting point, complemented by microcreep tests. The interpretation of existing experimental data is often compromised by the absence of complementary information concerning the relaxation of the relevant elastic modulus. Moreover, such essentially isochronal measurements typically conducted over a wide range of increasing and then decreasing temperature are potentially compromised by significant ongoing microstructural evolution, especially during the heating cycle. Such complications are largely circumvented by the conduct of isothermal measurements over a broad frequency band at each of a series of fixed temperatures during staged cooling following high-temperature annealing ideally conducted near the melting point (e.g., Rivière [25]).

Information concerning both frequency (ω) and temperature (T) dependence of both dissipation and modulus from sub-resonant forced-oscillation tests can potentially be analysed with long-established, but rarely used, procedures (Nowick and Berry [11]) for the incorporation of a distribution of relaxation times. Appropriate distributions $D(\tau)$ of relaxation times τ , embedded within a suitable creep function, provide an internally consistent way of modelling dissipation peaks, that are typically broader than the Debye peak of the standard anelastic solid [11,12], and also the high-temperature background [26], along with the associated modulus dispersion. Such an approach avoids *a priori* and subjective separation of background and peak dissipation, and provides a more comprehensive, albeit phenomenological, description of the viscoelastic relaxation than commonly used alternatives such as

$$Q^{-1} = [\omega\tau(T)]^{-n} = [\omega\tau_0 e^{E/(RT)}]^{-n} \quad (1)$$

(e.g., Schoeck et al. [27]) which are adequate approximations to the background dissipation only for more limited ranges of frequency and temperature.

Complementary microcreep tests allow the distinction to be made between recoverable (anelastic) and permanent viscous strains [11]. Such tests also have the potential to constrain the stress-strain relationship and underlying deformation mechanisms at lower stresses than conventional deformation measurements.

The first objective of the present paper is to report new measurements of

internal friction and dynamic moduli obtained on three polycrystalline pure copper specimens, over the complete mHz-Hz range, from annealing temperature down to room temperature. In addition to data for two new specimens annealed at 1050 °C, results are reported here of an exploratory study of a copper specimen annealed at 900 °C, that were used by Jackson et al. [28] to model the viscoelasticity of copper jackets enclosing rock specimens tested in our laboratory. Measurements were obtained with the alternative torsional and flexural forced-oscillation strategies as in Jackson et al. [28], and taken in the linear viscoelastic regime, whose threshold was determined by performing forced-oscillation tests at varying strain amplitudes. Complementary microcreep tests allow documentation of that part of the inelastic strain that is recoverable. The extensive dataset now allows for robust fitting of a Burgers model for viscoelastic rheology to the shear modulus and internal friction data. A discussion is given on the non-linear viscoelastic behaviour found in copper, and on the occurrence and characteristic feature of the observed high-temperature peak. The determined values for the internal friction peak relaxation times and activation energy are compared to previous results, after which possible relaxation mechanisms are finally discussed.

2. Experimental materials and methods

2.1. Specimen materials

Starting material. Three cylindrical specimens of identical dimension (11.50 mm dia. \times 30.00 mm length) were machined from a pure polycrystalline copper rod (of unknown origin). The copper tubing (11.50 mm ID, 0.35 mm wall thickness) used to enclose the specimens for the experiments at high pressure and high temperature was drawn and supplied by Uniform Tubes Inc. of Collegeville, Pennsylvania. The starting specimen is mostly formed of equant grains of average size of around 50 μm (Fig. 1b), but also of regions having larger grains and lamellae of 100 μm (Fig. 1a). The starting jacket material contains small equant grains of average size of around 10 μm , with some concentric and presumably substantial longitudinal elongation (Fig. 1c). Chemical analysis using Laser Ablation Inductively Coupled Plasma Mass Spectrometry (LA-ICP-MS) reveals minor and comparable concentrations of impurities in specimen and jacket (see Table A.1).

Microstructures developed in the annealed specimens. Each specimen, enclosed within a copper jacket, was annealed *in situ* within the argon pressure medium of the apparatus described in Section 2.2.1 for mechanical testing at high pressure and temperature. The commercial high-purity argon (99.997 %) was stripped of any moisture (<10 ppm) or oxygen (<5 ppm) by the Mo furnace windings.

Table 1

Summary of experimental conditions on the three copper specimens. Specimens were tested in the experimental run number order.

Experimental run	Hydrostatic pressure, MPa	Annealing temperature, °C	Annealing duration, h	Grain size, mm	Shear stress amplitude, kPa
1390	200	900	27	0.05–3	1000 (= 8 σ_0)
1457	200	1050	15	3–12	250 (= 2 σ_0)
1609	200	1050	33	1–12	125 (= σ_0)

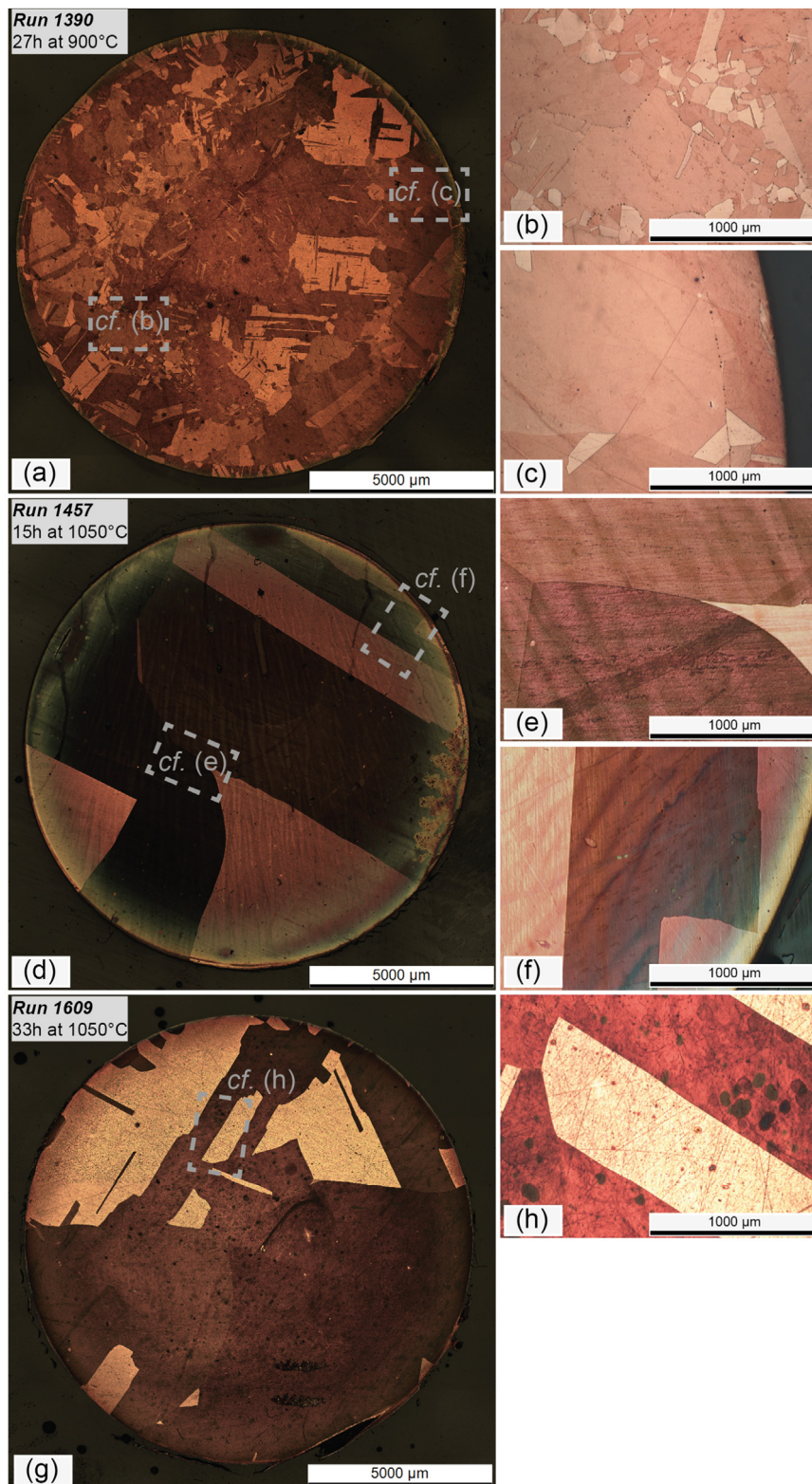


Fig. 2. Reflected light micrographs showing transverse sections of the three jacketed specimens as recovered after annealing at high temperature (see [Table 1](#)) and staged cooling. Polished sections were prepared using an identical technique as described in [Fig. 1](#) for starting material. (a,d,g): entire cross-sections of jacketed specimen; (b,e,h): interior of specimen; (c,f): jacket-specimen boundary.

Exposure to high temperature annealing (*cf.* [Table 1](#)) and subsequent staged cooling has resulted in very pronounced grain growth ([Fig. 2](#)). The jacketed specimen recovered from experimental run 1390 to a maximum temperature of 900 °C at 200 MPa ([Fig. 2a–c](#)) varies widely in grain size from 50 μm in a few portions — presumably relics

of the starting material — through lamellae with lengths of 100 s μm, to much large grains reaching 3 mm in dimension typically bounded by planar, presumably crystallographically-controlled, surfaces and by curved boundaries apparently pinned by impurities. The interface between the specimen and the enclosing jacket is defined by a semi-

continuous array of grain boundaries, with few grains bridging the interface. The jacket is also coarse-grained ranging up to a maximum of 350 μm , being the jacket thickness.

The jacketed specimens recovered from experimental runs 1457 and 1609, exposed to prolonged annealing at 1050 $^{\circ}\text{C}$ at 200 MPa have become much more coarse grained (Fig. 2d–h). Typically the cross-section of the jacketed specimen of 12.20 mm diameter contains no more than ten grains, in some cases spanning the entire diameter. Grain growth has erased most evidence of the interface between specimen and jacket, now marked only by an array of impurities.

2.2. Experimental technique and data analysis

2.2.1. Torsional forced-oscillation tests

Torsional forced-oscillation experiments were conducted under conditions of 200 MPa pressure and high temperatures in an apparatus described in detail elsewhere [29]. The confining pressure is applied by means of argon gas, within which an internal furnace provides access to a homogeneous temperature profile within $\pm 10^{\circ}\text{C}$ along the specimen. Specimens of 11.50 mm diameter and 30 mm length are clamped between rods of “Lucalox” high-grade polycrystalline alumina (General Electric Lighting, Cleveland, Ohio), tapered between 11.50 and 15.00 mm. Such an assembly is enclosed within a thin-walled (0.35 mm) copper jacket, sealed with an O-ring at each end against the argon confining gas. A normal stress equal to the confining pressure, acting across the interfaces between the optically flat surfaces of adjacent components, ensures effective frictional coupling.

A sinusoidally time-varying torque is applied at ten oscillation periods, approximately equally spaced between 1 and 1000 s, by a pair of electromagnetic drivers located at the lower end of the assembly (see, for instance, Fig. 1a of Cline and Jackson [30]). The adjustable torque amplitude is typically equivalent to a maximum shear stress in the range 60–500 kPa, resulting in maximum shear strains in the range $3 - 30 \times 10^{-6}$ at the highest temperature and 100 s oscillation period. Time-varying displacements are measured by pairs of parallel-plate capacitance transducers mounted off-axis for mechanical advantage. Examples of raw data are given in Jackson and Paterson [29].

A brief summary of the main steps of data processing strategy, details of which can be found in Jackson and Paterson [29] and Jackson et al. [31], is given here. At each oscillation period, the modulus and phase of the ratio of the complex time-dependent distortions of the specimen assembly and the hollow steel elastic standard, maintained at room temperature and connected mechanically in series, are termed the “normalised torsional compliance” and “specimen assembly phase lag”, respectively. Subsequent extraction of shear modulus G and internal friction Q_G^{-1} for the copper specimen itself requires the conduct of a parallel series of experiments on a “reference assembly” in which the copper specimen is replaced by a control specimen of single-crystal sapphire (of the same dimension), for which the temperature-dependence of elastic constants is known [28]. As all elements in the assembly are connected mechanically in series and subjected to the same low-frequency oscillating torque, subtraction of the complex compliance for the reference assembly from that of the specimen assembly removes all contributions from the jacketed alumina and steel rods [29]. Accordingly, the compliance differential describes the behaviour of the jacketed copper specimen relative to that of similarly jacketed sapphire. As viscoelasticity of the jacket is itself an unknown, final extraction of viscoelastic properties for the copper specimen requires trial values of these quantities for the copper jacket, with iteration to consistency between the resulting values of shear modulus and internal friction for the copper specimen and those of the jacket material [32]. Examination of microstructures in recovered specimens after annealing and staged cooling (Fig. 2) indicates that the underlying assumption that copper jacket and specimen have the same viscoelastic properties is reasonable, given broadly similar microstructures after high-temperature annealing and staged cooling.

2.2.2. Flexural forced-oscillation tests

Recent modifications of the apparatus allow for measurements also of Young's modulus E and its associated internal friction Q_E^{-1} by subjecting the assembly to flexural-mode forced-oscillation [33]. Access to this alternative mode involves switching of the electromagnetic drivers and displacement transducers to measure flexural displacements under a sinusoidally varying bending force (see Fig. 1c of Cline and Jackson [30]) — in the same frequency range as for torsional oscillations. Examples of raw data can be found in Jackson et al. [33]. The result of a given measurement is expressed as a normalised and dimensionless “complex flexural compliance”, as described above for torsional-mode oscillations. However, in contrast with torsional oscillations, the procedure used to subsequently extract specimen's Young's modulus and its associated internal friction does not involve the comparison with a parallel experiment on a “reference assembly”, but instead requires direct inversion through the use of a finite-difference filament elongation model for flexure of the long thin experimental assembly [33]. This model has been recently modified by Cline and Jackson [30] to accommodate an applied bending force rather than bending moment, and to account for high-temperature viscoelasticity. The complex Young's modulus is estimated from the complex shear modulus derived from torsional forced oscillation measurements at the same conditions of temperature and oscillation period, and a real, anharmonically temperature-dependent bulk modulus. The parallel configuration of capacitance displacement transducers for the torsional mode discriminates strongly against the mainly flexural disturbance of the specimen assembly by the dense gas pressure medium undergoing vigorous thermal convection [29]. However, such discrimination against flexural noise is unavailable for the corresponding flexural mode measurements — resulting in increased scatter, especially of the small phase lags.

2.2.3. Torsional microcreep tests

Torsional forced-oscillation measurements provide no direct opportunity to document the fraction of inelastic strain that is recoverable, *i.e.*, anelastic as defined by Nowick and Berry [11], upon removal of the applied torque. However, such information is accessible through complementary torsional microcreep tests, consisting of five segments — each typically of 2000 s duration and constant torque with successive amplitudes $[0, +L, 0, -L, 0]$ [29]. The first segment is used to estimate and correct for any linear drift, leaving a four-segment record within which the torque is switched at times t_i , where $i = 1, \dots, 4$. The switching of the torque can be modelled by Heaviside step functions of appropriate sign s_i (equal to $+1$ at t_1 and t_4 , and to -1 at t_2 and t_3). In the absence of microcreep data for the appropriate (copper-jacketed sapphire) reference assembly, processing of the microcreep data for the copper-jacketed copper specimens of this study cannot proceed exactly as recommended by Barnhoorn et al. [34]. Instead, the time-dependent torsional distortion (*i.e.*, twist) of the assembly dominated by that of the copper specimen, rather than the difference between creep records for specimen and reference assemblies, is fitted to a function $S_{\text{fit}}(t)$ that is the superposition of the responses to each of the torque switching episodes prior to the i^{th} segment of the record (where $i = 1, \dots, 4$), prescribed by the Andrade creep function $J(t'_i)$:

$$S_{\text{fit}}(t) = \sum_{i=1}^k s_i J(t'_i), \quad (2)$$

where t'_i is the time elapsed since the i^{th} switching of the torque. As in Barnhoorn et al. [34], the Andrade creep function is given by

$$J(t') = J_U + \beta t'^m + t'/\eta_A, \quad (3)$$

where the first, second and third terms on the right-hand side represent the instantaneous elastic response, and the recoverable (anelastic) and permanent contributions to the inelastic strain, respectively. The fraction f_R of the inelastic strain that is recoverable is thus estimated as a function of the duration t of loading as

$$f_R = \beta t^n / (\beta t^n + t/\tau_A) = 1/[1 + t^{1-n}/(\beta\tau_A)]. \quad (4)$$

2.3. Experimental procedure

Each of the three copper specimens was loaded into the gas apparatus, pressurised ultimately to a confining pressure of 200 MPa, and heated to the desired annealing temperature at a rate of 450 °C per hour followed by sustained exposure to the highest temperature (*cf.* Table 1). During such annealing, several torsional forced-oscillation tests, at various strain amplitudes, were performed to check for both *temporal evolution* and *amplitude dependence* of mechanical behaviour (*cf.* Section 3.1.1). The cessation of temporal evolution — and of microstructural evolution presumed responsible for it — justifies the commencement of staged cooling, during which torsional and flexural forced-oscillation as well as torsional microcreep measurements were taken at selected temperatures down to room temperature. After completion of a campaign of mechanical measurements at a given temperature, typically requiring 5–15 h, the next temperature was reached using a ramp of 450 °C per hour. After completion of measurements at room temperature, a *revisit* of the highest temperature documents any change in mechanical behaviour attributable to further microstructural evolution during staged cooling. After completion of the experiment, jacketed specimens were sectioned for examination of microstructures (Fig. 2).

2.4. Burgers model for viscoelastic relaxation

Torsional forced-oscillation tests provide shear modulus and internal friction (G , Q_G^{-1}) data at selected periods for given temperatures, as described in Sections 2.2.1 and 2.3. Such a dataset with a priori errors $\sigma(G)/G = 0.03$ and $\sigma(\log Q^{-1}) = 0.05$, has been fitted by a “background plus peak” model for linear viscoelasticity based on a Burgers-type creep function [35]:

$$J(t) = J_U \left[1 + \Delta \int_0^\infty D(\tau)(1 - e^{-t/\tau})d\tau + t/\tau_M \right] \quad (5)$$

where J_U is the unrelaxed compliance, Δ the anelastic relaxation strength, $\tau_M = \eta J_U$ the Maxwell time for viscous relaxation, and $D(\tau)$ a suitable distribution of anelastic relaxation times. The use of a creep function guarantees an internally consistent description of the variations of dissipation and modulus dispersion with oscillation period T_0 or angular frequency $\omega = 2\pi/T_0$, through the real $J_1(\omega)$ and negative imaginary $J_2(\omega)$ parts of the associated complex compliance $J^*(\omega)$:

$$G(\omega) = [J_1^2(\omega) + J_2^2(\omega)]^{-1/2} \quad \text{and} \quad Q^{-1} = J_2(\omega)/J_1(\omega) \quad (6)$$

[11]. The Burgers model incorporates a broad distribution $D_B(\tau)$ of anelastic relaxation times, used for modelling high-temperature *monotonic background dissipation*, specified as:

$$D_B(\tau) = \frac{\alpha\tau^{\alpha-1}}{\tau_M^\alpha - \tau_L^\alpha} \quad (7)$$

with an associated relaxation strength Δ_B , and $0 < \alpha < 1$, for $\tau_L < \alpha < \tau_M$ and zero elsewhere [26]. An anelastic *dissipation peak*, superimposed upon the monotonic background, is modelled by inclusion of a separately normalised distribution of relaxation times

$$D_P[\ln(\tau)] = \frac{e^{-(1/2)[\ln(\tau/\tau_P)/\sigma_P]^2}}{\sigma_P\sqrt{2\pi}} \quad (8)$$

with an associated relaxation strength Δ_P and a characteristic relaxation time τ_P for the peak [11]. In addition, the upper limit for the broad distribution of anelastic relaxation times (Eq. (7)), τ_M , is identified with the characteristic time $\tau_M = \eta J_U$ for the Maxwell relaxation, giving way to *viscous relaxation* at sufficiently long timescales $t \gg \tau_M$.

The temperature dependence of each of the characteristic relaxation times (τ_L , τ_M , τ_P), relative to their respective values (τ_{LR} , τ_{MR} , τ_{PR}) at

reference temperature T_R , follows the Arrhenian expression

$$\tau_i(T) = \tau_{iR} \left[e^{\left(\frac{E_i}{R}\right)\left(\frac{1}{T} - \frac{1}{T_R}\right)} \right], \quad (9)$$

where $i = L$ or $i = M$ for the broad anelastic relaxation background, associated with an activation energy E_B ; and where $i = P$ for the anelastic relaxation peak, associated with an activation energy E_P ; R is the gas constant.

The last two adjustable parameters describing the extended Burgers model are the anharmonic or unrelaxed shear modulus $G_U(T_R)$ at the reference temperature, and its temperature derivative dG_U/dT , which allow to specify the temperature dependence of the unrelaxed compliance $J_U = 1/G_U$ simply as

$$G_U(T) = G_U(T_R) + (T - T_R) \frac{dG_U}{dT}, \quad (10)$$

which implicitly assumes that dG_U/dT is temperature-independent.

3. Results

3.1. Torsional forced-oscillation tests

3.1.1. Temporal evolution and linearity of viscoelastic behaviour

Specimens annealed at 1050 °C. The temporal evolution of the viscoelastic behaviour during high-temperature annealing, and its sensitivity to strain amplitude, are assessed from the compliance of the entire specimen assembly, rather than the shear modulus calculated for the specimen itself. Thus the quantities plotted in Fig. 3 are the modulus and negative phase of the (complex) ratio of the torsional distortion (twist) of the specimen assembly and that of the elastic standard.

Mechanical testing during sustained annealing (33 h) of the copper specimen at the highest temperature of 1050 °C in experimental run 1609 provides evidence of decreasing compliance and phase lag over time, suggestive of microstructural evolution of the copper specimen. Such evolution is most clearly revealed by comparing results obtained at stress amplitude $\sigma_0 = 125$ kPa after 5 and 25 h exposures (Figs. 3a and b). In contrast, the general consistency of the results obtained after 10 h and 25 h of exposure at stress amplitudes of $\sigma_0/2$ and σ_0 respectively, suggests that temporal evolution of mechanical behaviour, and the microstructural evolution (grain growth) presumed responsible for it, are essentially complete - justifying the commencement of staged cooling. Subsequent tests during staged cooling reveal no evidence of ongoing temporal evolution, *e.g.*, Figs. 3c and d for tests at 1000 °C, suggesting that the annealed microstructure remains stable during staged cooling. Under these circumstances, we expect to infer, by comparison of the torsional compliances of the specimen and reference assemblies, values of shear modulus and strain energy dissipation representative of the stable microstructure.

The strategy of doubling or halving the applied torque reveals linearity of viscoelastic behaviour for stress amplitudes $< \sigma_0$. Closely consistent results are obtained at maximum stress amplitudes σ_0 and $\sigma_0/2$ (Fig. 3). In contrast, results at higher stress amplitude $2\sigma_0$ yield consistently higher torsional compliance and phase lag at 1050 °C (Figs. 3a and b), although results are also affected by temporal evolution as previously noted. However, such strain amplitude-dependent behaviour is clearly observed at lower temperatures of 1000 °C (Figs. 3c and d), and also at 700 and 400 °C. Accordingly, the maximum shear stress amplitude σ_0 was employed during staged cooling to room temperature.

A higher standard stress amplitude $2\sigma_0$ was used for the copper specimen annealed at 1050 °C, during experimental run 1457. Although no tests were conducted at lower stress amplitudes for this specimen, comparison of results for tests at stress amplitude $4\sigma_0$ yielded markedly higher compliance and phase lag at 1000 °C and below. Based on the results for the other specimen annealed at 1050 °C (see above), experimental run 1457 should be regarded as *marginally* probing the non-

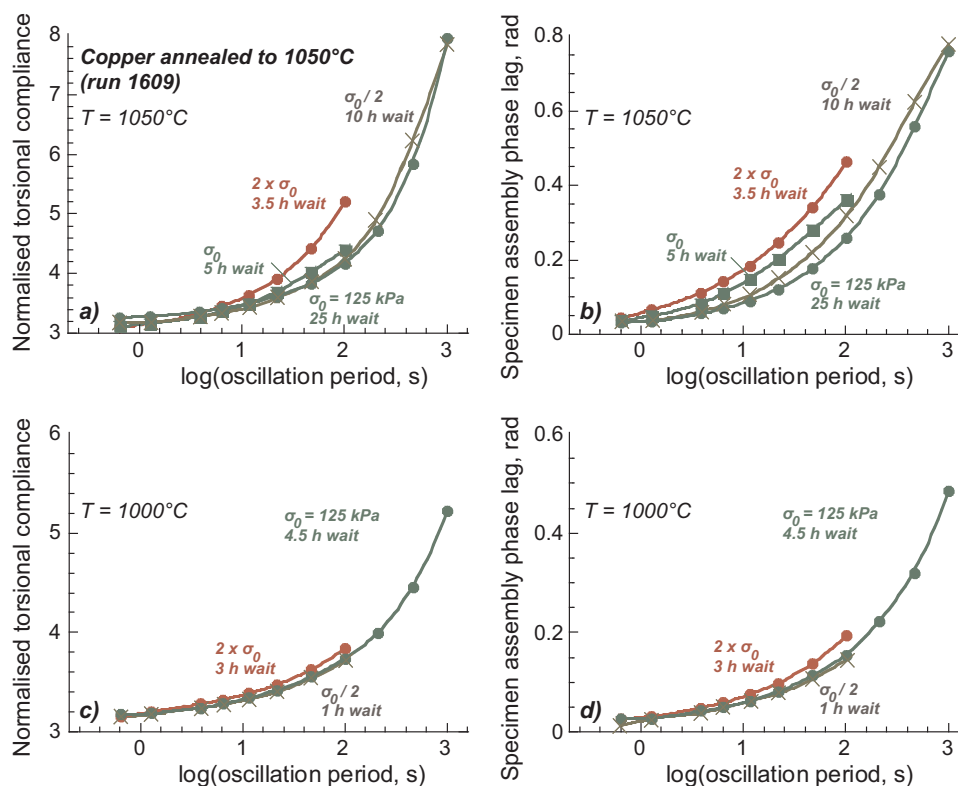


Fig. 3. Results of torsional forced-oscillation tests, for the specimen assembly containing the copper specimen annealed at 1050 °C during 33 h (experimental run 1609), documenting temporal evolution and strain amplitude dependence of the mechanical behaviour with increasing exposure. a,b) 1050 °C; c,d) 1000 °C.

linear viscoelastic regime. Evidence for essentially complete microstructural evolution after 15 h annealing at 1050 °C comes from the reproducibility of viscoelastic behaviour while revisiting the 1050 °C temperature following staged cooling to room temperature, and by the strong similarities in microstructures of the recovered specimens that were annealed at 1050 °C (Fig. 2).

Specimens annealed at 900 °C. Results for this early exploratory study are presented in the appendix.

3.1.2. Shear modulus and internal friction for individual specimens

Specimens annealed at 1050 °C. Experimental results for the variation of shear modulus and internal friction with oscillation period and temperature are shown in Figs. 4 and 5. Experimental run 1609 (Fig. 4; cf. Table 1) is regarded as providing the most reliable and preferred dataset in this study, as it satisfies both conditions of complete microstructural evolution upon long annealing duration, and mechanical testing at small strains in the linear regime (Section 3.1.1). Data for this specimen reveal highly systematic variation of both shear modulus and internal friction with oscillation period and temperature (Fig. 4). At the highest temperatures (Figs. 4a,b), shear modulus decreases markedly with increasing oscillation period, but the strength of such dispersion decreases consistently with decreasing temperature. Internal friction varies monotonically with period and temperature for temperatures above 850 °C. At lower temperatures, a broad internal friction peak of moderate amplitude enters the observational window from shorter periods (located at about 700 °C at 1.28 s) and moves systematically to longer periods with decreasing temperature (Figs. 4b,d). Superposition of the broad peak upon the period-dependent monotonic background creates a well-defined “plateau”, of almost temperature- and period-independent Q_G^{-1} , at temperatures between 700 and 500 °C for the experimentally accessible periods of 1–1000 s.

The specimen of experimental run 1457, despite a shorter annealing time at 1050 °C, and larger strain amplitudes by a factor of 2 — *i.e.*, implying conditions of marginally non-linear behaviour —, shows

strong similarities with experimental run 1609, over the entire range of oscillation period and temperature (Fig. 5). Minor differences between the results for the two specimens include a tendency towards somewhat lower shear modulus and higher internal friction in experimental run 1457, and some modest differences in shear modulus and internal friction at temperatures below 400 °C.

Specimen annealed at 900 °C. Results for this early exploratory study are presented in Appendix.

3.1.3. Burgers model for viscoelastic relaxation in copper

An extended Burgers model (*cf.* Section 2.4) has been fitted to each of the torsional forced-oscillation datasets (Figs. 4, 5 and A.1; fitting parameters in Table 2). For the two specimens annealed at 1050 °C, the model associated with the curves in Figs. 4–5 evidently provides a generally satisfactory description of the observed variations of modulus and dissipation over a wide range of conditions (350–1050 °C, 1–1000 s). In particular, the model captures the key observation that the broad internal friction peak and associated modulus dispersion traverses the observational oscillation period window from shorter to longer periods with decreasing temperature. However, for experimental run 1609 (1457), as temperature decreases below 400 (300) °C, the model systematically underestimates the observed dissipation — initially at short periods but ultimately across the entire observational window — suggestive of an additional low-temperature peak of modest height that is not captured by the model. For the exploratory study on the specimen annealed at 900 °C (Fig. A.1), the height and position of the high-temperature dissipation peak are poorly resolved due to sparse sampling of experimental data, in the temperature interval 200–600 °C.

3.2. Flexural forced-oscillation tests

Specimens annealed at 1050 °C. For the two specimens annealed at 1050 °C, flexural forced-oscillation data, in the form of “normalised flexural compliance” and “specimen assembly phase lag” obtained at

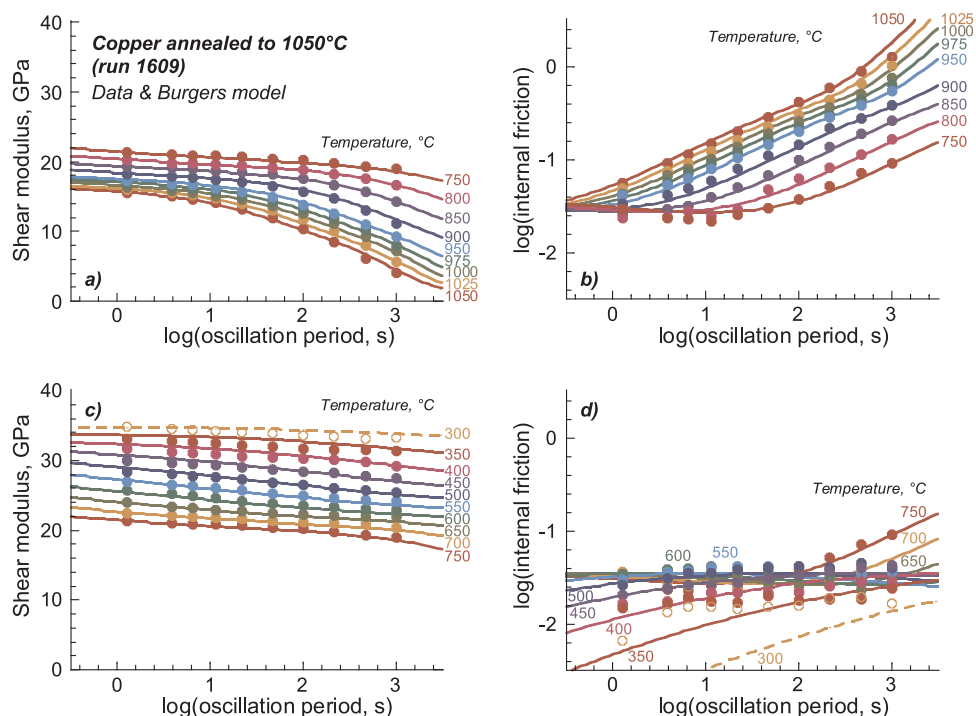


Fig. 4. Shear modulus and internal friction (G, Q_G^{-1}) data (symbols colour-coded for temperature) for the copper specimen annealed at 1050 °C during 33 h (experimental run 1609), and optimal Burgers “background + peak” model (colour-coded curves) fitted to $N = 166$ (G, Q_G^{-1}) data pairs (i.e., all data for temperatures between 1050 and 350 °C) with misfit $\sqrt{\chi_{\text{tot}}^2}/(2N) = 1.05$. Shear stress amplitude is $\sigma_0 = 125$ kPa, corresponding to maximum shear strains of 16×10^{-6} , 6×10^{-6} and 3×10^{-6} at 1050 °C, 900 °C and 600 °C, respectively, at the 1000 s longest oscillation period.

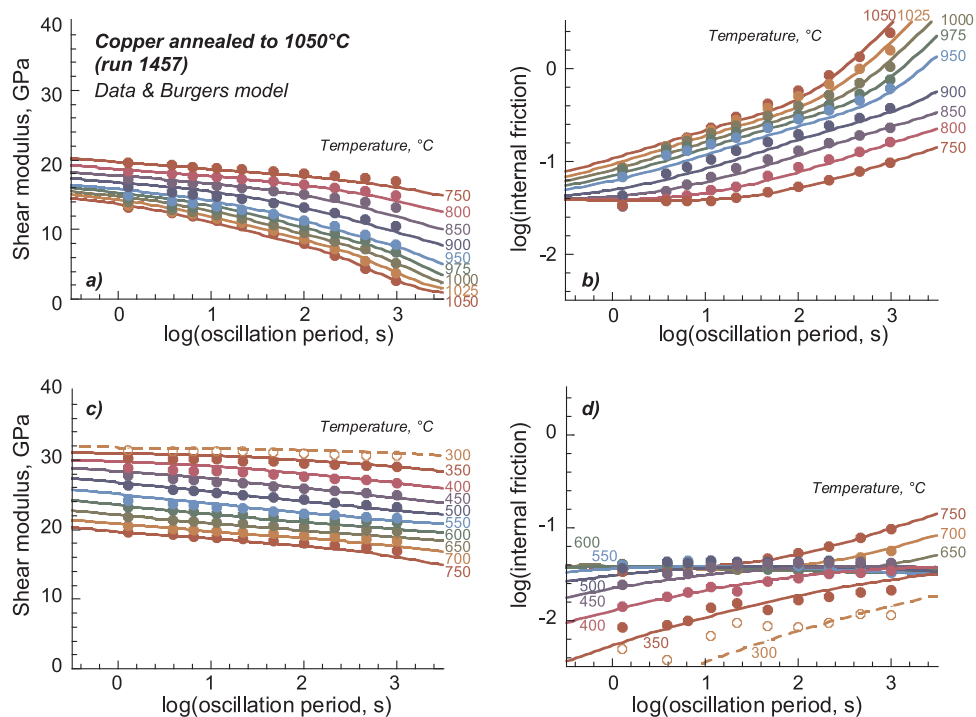


Fig. 5. Shear modulus and internal friction (G, Q_G^{-1}) data (symbols colour-coded for temperature) for the copper specimen annealed at 1050 °C during 15 h (experimental run 1457), and optimal Burgers “background + peak” model (colour-coded curves) fitted to $N = 170$ (G, Q_G^{-1}) data pairs (i.e., all data for temperatures between 1050 and 350 °C) with misfit $\sqrt{\chi_{\text{tot}}^2}/(2N) = 0.91$. Shear stress amplitude is $2\sigma_0 = 250$ kPa, corresponding to maximum shear strains of 48×10^{-6} , 13×10^{-6} and 7×10^{-6} at 1050 °C, 900 °C and 600 °C, respectively, at the 1000 s longest oscillation period.

representative temperatures within the range 400–1050 °C are displayed in the left-hand panels of Fig. 6. Such data are significantly more scattered than torsional forced-oscillation data as explained previously

(Section 2.2.2); the scatter provides an indication of the experimental uncertainties. Nevertheless, it is clear that the normalised flexural compliance of the specimen assembly increases systematically with

Table 2

Details of extended Burgers model fitted to N (G , Q_G^{-1}) data pairs for three copper specimens (see Table 1), showing best refined values for the 11 model parameters, and misfit ($\chi_{\text{tot}}^2 = \chi_G^2 + \chi_{Q_G^{-1}}^2$). Parameter uncertainties are parenthesised after parameter value, and bracketed model parameters indicate fixed parameter values, for purposes of convergence in fitting strategy. For a description of model parameters, see Section 2.4.

Experimental run	1390	1457	1609
T_R , K	973.0	973.0	973.0
N	83	170	166
G_U , GPa	31.0(0.6)	26.5(0.3)	27.9(0.3)
dG_U/dT , MPa K ⁻¹	- 16.3(0.8)	- 13.2(0.7)	- 17.2(0.5)
Δ_B	1.14(0.09)	1.35(0.04)	1.05(0.3)
α	0.422(0.017)	0.434(0.015)	0.632(0.022)
$\log(\tau_{LR})$, s	[0]	[- 2]	[- 2]
$\log(\tau_{MR})$, s	3.66(0.06)	5.03(0.06)	4.61(0.05)
Δ_P	0.34(0.04) ^a	0.45(0.03)	0.38(0.02)
$\log(\tau_{PR})$, s	- 2.70(0.24) ^a	- 1.41(0.14)	- 1.43(0.10)
σ_P	5.2(0.5) ^a	5.9(0.3)	5.6(0.3)
E_B , kJ mol ⁻¹	159(4)	263(5)	213(4)
E_P , kJ mol ⁻¹	111(9) ^a	203(9)	195(8)
χ_G^2	71.9	162.4	70.8
$\chi_{Q_G^{-1}}^2$	83.2	209.7	205.3
χ_{tot}^2	155.1	372.1	276.1
$\sqrt{\chi_{\text{tot}}^2/(2N)}$	0.97	1.05	0.91

^a Indicative value since the peak is poorly resolved by the data.

increasing temperature, and at temperatures greater than 900 °C, with increasing oscillation period. Correspondingly, the specimen assembly phase lags are about 0.005 rad for temperatures of 400–650 °C, but increase significantly and become period-dependent at higher temperatures reaching 0.04 rad at 1050 °C and 100 s oscillation period.

The results of modelling the complex Young's modulus as described in Section 2.2.2 are displayed in the right-hand panels of Fig. 6. It is evident that the model, which combines torsional oscillation data for the complex shear modulus with the real anharmonic bulk modulus, reproduces reasonably faithfully the broad trends for normalised flexural compliance and specimen assembly phase lag, although both

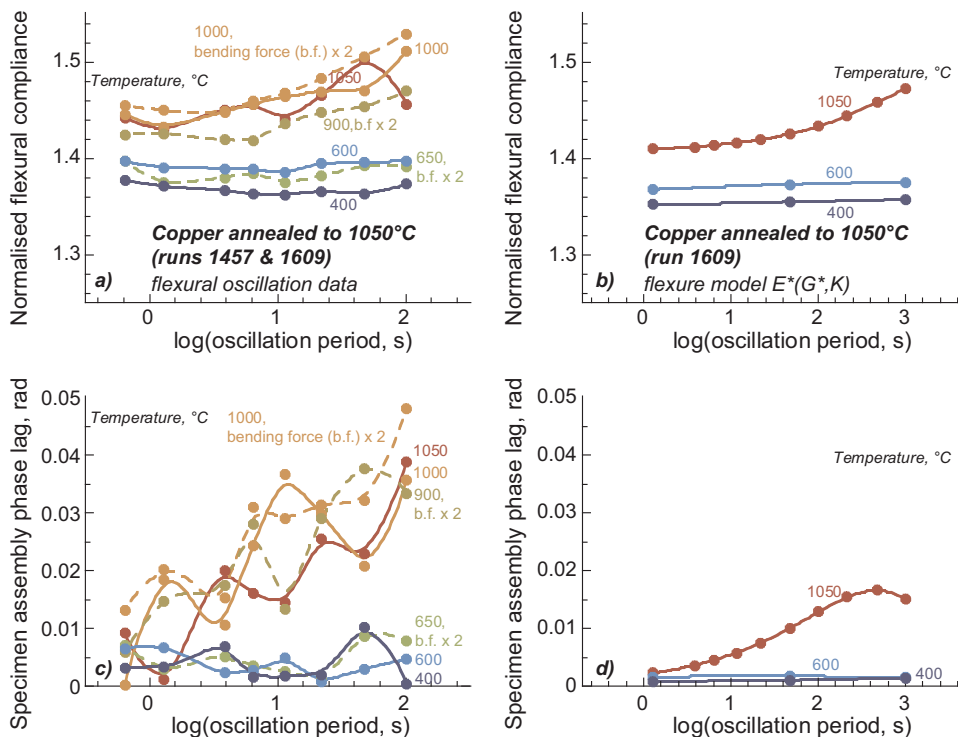


Fig. 6. Normalised flexural compliance and phase lag data (left-hand panels) and flexure model for complex Young's modulus (right-hand panels), for the specimen assembly (cf. Section 2.2.2 for details) containing the copper specimen annealed at 1050 °C (in experimental run 1457 or 1609, see Table 1). At 1050 °C and 101 s oscillation period, maximum flexural strain amplitudes are 0.8×10^{-6} and 1.6×10^{-6} for experimental runs 1609 and 1457, respectively. The curves in the left-hand panels are intended only to indicate the broad trends among scattered data (see text).

quantities are somewhat underestimated at the higher temperatures and longer periods.

Specimens annealed at 900 °C. Results for this early exploratory study are presented in the appendix.

3.3. Representative results for complementary torsional microcreep tests

Representative data from the complementary torsional microcreep tests, conducted at temperatures within the high-temperature viscoelastic regime, are presented in Fig. 7. It is immediately evident that, at the highest temperatures, the time-dependent torsional distortion of the assembly, dominated by the deformation of the copper specimen, dwarfs the instantaneous elastic response, and that a substantial fraction of this inelastic strain is recoverable upon removal of the applied torque. The 2000 s duration of each segment is clearly insufficient to allow the process of recovery of the anelastic strain to reach completion. The amplitude of the inelastic deformation decreases systematically with decreasing temperature. For temperatures ≤ 900 °C, an adequate fit to the Andrade model (Eqs. (2) and (3)) was obtained for the entire 4-segment record of 8000 s duration sampled at 1 Hz (i.e., $N = 8000$ $S(t)$ data) with values of $(\chi^2/N)^{1/2} \sim 1$ with $\sigma(S) = 10^{-4}$ rad/Nm. However, for higher temperatures, it proves impossible to obtain a satisfactory fit for the entire record, probably because of inadequate modelling of drift. Under these circumstances, a much more satisfactory fit was obtained by excluding the final two segments of the microcreep record as shown in Fig. 7. Andrade fitting parameters are given in Table A.2.

The optimal Andrade model parameters associated with either 4- ($N = 8000$) or 2- ($N = 4000$) segment fits are used to estimate the fraction f_R of recoverable non-elastic strain (Eq. (4)). The Andrade model parameter β increases systematically, whereas the parameter η_A decreases systematically, with increasing temperature. The product $\beta\eta_A$ is therefore much less temperature-sensitive, as is the exponent n . Consequently, the fraction f_R of recoverable inelastic strain varies similarly with loading duration for all temperatures within the range 800–1050 °C (Fig. 7c). That f_R becomes generally less than 0.5 for loading durations greater than 1000 s, attests to dominantly anelastic (viscous) behaviour for shorter (longer) loading periods.

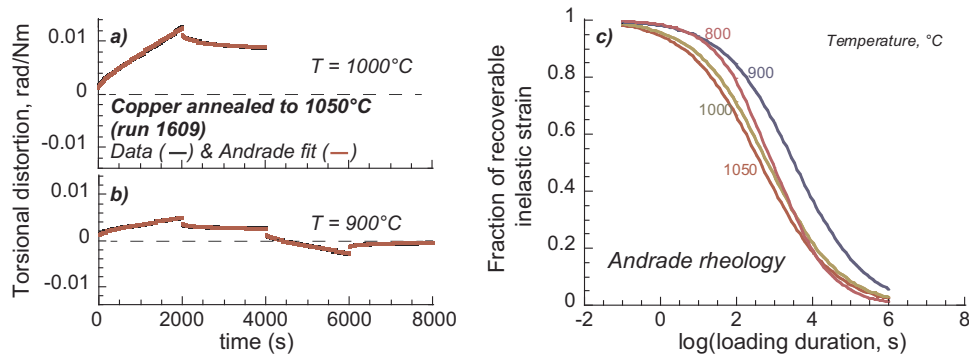


Fig. 7. Torsional microcreep records and essentially indistinguishable Andrade fits, for the copper specimen annealed at 1050 °C during 33 h (experimental run 1609), at two representative temperatures: a) 1000 °C (misfit: $\sqrt{\chi_{\text{tot}}^2}/(N) = 1.18$); b) 900 °C (misfit: $\sqrt{\chi_{\text{tot}}^2}/(N) = 0.75$). c) Fraction of recoverable inelastic strain vs. loading duration at high temperatures.

4. Discussion

4.1. Strain-dependent dynamic modulus and internal friction in copper

It is well known that dynamic moduli and internal friction of polycrystalline copper, and generally of polycrystalline fcc metals, are very sensitive to strain amplitude even at small strains. The experimental results of Weinig and Machlin [3] on dilute alloys of copper demonstrate non-linear behaviour at strain amplitudes above 10^{-5} . Woïrgard et al. [23] and Rivière et al. [21] report non-linear behaviour even at strains below 10^{-6} on aluminium, silver and nickel. For the torsional and flexural forced-oscillation tests of the present study, a torque or bending stress of the same amplitude is applied at each temperature, yielding temperature- (and period-) dependent strains (exemplified, at representative temperatures and 1000 s oscillation period, in captions of Figs. 4, 5 and A.1 for the three specimens). Variation of torque amplitude at selected temperature (Section 3.1.1) reveals that the threshold for non-linearity of viscoelastic behaviour in the three annealed copper specimens is near 5×10^{-6} .

In the regime of non-linear viscoelasticity, increasing strain amplitudes are expected to result in decreasing dynamic modulus and increasing internal friction [36,23]. This is clearly observed in the present measurements (e.g., Fig. 3), on all samples and at various temperatures — leading to the strategy of minimising strain amplitudes for specimen of experimental run 1609. In contrast, the other specimen annealed at 1050 °C (experimental run 1457) was tested in conditions of marginally nonlinear behaviour. Despite these differences, a very close consistency of shear modulus and internal friction is found on these two specimens, that differ only in the duration of annealing (Table 1).

The use of a creep function to model the observed variations of both modulus and dissipation ensures compliance with the Kramers-Kronig relations of linear viscoelasticity. The model adequately captures temperature and period variations of shear modulus and internal friction for each of the three specimens, even for marginally non-linear viscoelasticity, without significant differences in misfit (Table 2). It is accordingly concluded that non-linear effects are only modest in the range of strain amplitudes used in this study.

4.2. Viscosities inferred from torsional oscillation and microcreep tests: evidence for Harper-Dorn creep?

The Andrade model fits of microcreep records (at high-temperatures) indicate a notable contribution of viscous behaviour at loading durations greater than 100 s. Hence, it is reasonable to extract values of viscosity from the Burgers model fitted to torsional forced-oscillation data, where $\eta(T) = \tau_M(T)G_U(T)$ at a given temperature — using Eq. (9) and the anharmonic temperature derivative dG_U/dT in Table 2. In the high-temperature range, inferred viscosities are $\eta = 1.3 \times 10^{12}$ and

1.4×10^{13} Pas at 1050 and 900 °C, respectively. The viscosity inferred from the Andrade fits to microcreep data is that for transient creep at comparably low strain amplitudes. The values of viscosity η_A given in Table A.2 can be directly converted to shear viscosity η as $\eta = (2l)/(\pi R^4)\eta_A$, where (l,R) are the length and radius of specimen, respectively. This yields $\eta = 1.6 \times 10^{12}$ and 1.8×10^{13} Pas at 1050 and 900 °C, respectively. Such values compare well from the ones inferred from the Burgers fit to the torsional oscillation data.

The Frost and Ashby [37] flow laws for power-law and diffusional creep at 1050 °C, using $\sigma/G_U = 5 \times 10^{-6}$ (a representative strain), $G_U = 25$ GPa, and grain size $d = 3$ mm, yield sub-equal estimated strain rates of $7.5 \times 10^{-11} \text{ s}^{-1}$ and $1.25 \times 10^{-10} \text{ s}^{-1}$, respectively — consistent with proximity of these conditions to the boundary between power-law and diffusional creep [37]. Of these, diffusional creep is more compatible with linear behaviour observed in the present study at low stress amplitudes. However, the viscosity (stress/strain rate) of 10^{15} Pas associated with the Frost-Ashby flow law is greater than that inferred from the present study by three orders of magnitude. Accordingly, it is speculated that Harper-Dorn creep, reported for other fcc metals and suggested to involve climb-controlled dislocation creep at constant dislocation density [37], may be involved in the low-strain mechanical tests of the present study. The dimensionless Harper-Dorn coefficient, required to match the observed strain rate at 1050 °C, is 1.3×10^{-10} , intermediate between those for Al and Pb, and consistent with a not unreasonable dislocation density of $3 \times 10^9 \text{ m}^{-2}$.

4.3. High-temperature anelastic relaxation peak(s) observed in copper

Anelastic relaxation peak “classification” in past experiments. Several experimental studies on copper have clearly demonstrated that annealing at increasingly high temperature generally produces a shift of internal friction peak(s) towards higher temperatures [2,38,14,23,9], associated with progressive disappearance of the “low” to “mid-temperature peaks” — in the terminology of Williams and Leak [13]. Each peak is notably characterised by its homologous temperature, being the ratio of its characteristic temperature T_p at a given frequency (usually 1 Hz) to the melting temperature T_F . The well-known low-temperature “grain-boundary peak” of Kê [2], typically found around 250–300 °C ($\sim 0.4 T_F$) in copper, gradually disappears upon medium to high-temperature annealing typically above 750–800 °C [38,21,9]. Several peaks are in fact superimposed in the $0.4\text{--}0.5 T_F$ region [15,21,8], some of which are artefacts of experimental testing conditions — notably strain amplitudes in pendulum experiments [17] — reconciling most differences in peak positions found by previous authors. The present discussion focuses on the occurrence and characteristic features of *high-temperature peak(s)*, as found in copper annealed at sufficiently high temperatures. Such conditions are satisfied for all three specimens in the present study, however, the more comprehensive data for the two

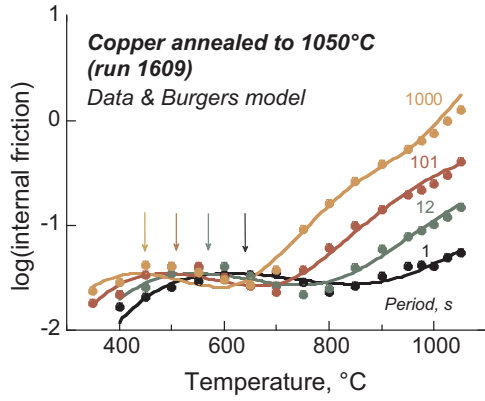


Fig. 8. Internal friction (in torsion) data (symbols colour-coded for oscillation period) and Burgers “background + peak” model (colour-coded curves) for copper specimen annealed at 1050 °C, at selected oscillation periods (arrows indicate approximate peak temperature at given oscillation period).

specimens annealed at 1050 °C will form the basis for the following discussion.

General features of the “high-temperature internal friction peak” in this study. The absence of strong low-temperature peaks in this study is in agreement with the aforementioned effect of high-temperature annealing on internal friction peaks in fcc metals. The “high-temperature peak” observed in this study is highlighted by displaying the torsional internal friction for the Burgers model as a function of temperature at selected periods between 1 and 1000 s on a specimen annealed at 1050 °C (Fig. 8). The broad dissipation peak moves systematically towards shorter oscillation period with increasing temperature from 1000 s near 450 °C to 1 s near 650 °C, as prescribed by Eq. (9) with the model parameters of Table 2.

DeMorton and Leak [38] first suggested that the *peak height* (closely related to the relaxation strength) is enhanced by the annealing temperature — and associated grain growth. Disappearance of the high-temperature peak, upon a very high-temperature annealing just below the melting temperature, has been reported in metals of high stacking fault energy such as aluminium [21] but not in copper [9]. The new results of this study on copper show that the peak amplitude is broadly comparable for all three samples (Table 2), even those annealed close to the melting point.

The comparison between the two copper specimens annealed at 1050 °C (experimental runs 1457 and 1609), which were tested under marginally non-linear and linear conditions, respectively, is useful to discuss the effect of strain amplitude on peak height but also *peak location*. Gaboriaud et al. [10] report measurements at various strain amplitudes in the range $6\text{--}30 \times 10^{-6}$ on a copper specimen alloyed with 13% aluminium, which suggest that non-linear effects change the peak amplitude, but not its position. The obtained values of relaxation time, $\log(\tau_{PR})$, and relaxation strength, Δ_P (Table 2), confirm that this is also the case for pure copper.

The other striking feature of the high-temperature peak observed for each specimen is its significant *width*, as revealed by the high values of parameter σ_P for the optimal Burgers models (Table 2). The log-normal distribution $D_P(\ln \tau)$ of relaxation times (Eq. (8)) used in the Burgers model results in a peak in $J_2[\log(\omega\tau_P)]$, and hence in $Q^{-1}[\log(\omega\tau_P)]$ (Eq. (6)). The peak is centred at $\omega\tau_P = 1$, and for non-zero σ_P , has a full width $\Delta[\log(\omega\tau_P)]$ at $1/e \times$ maximum height that is greater than that (1.14) for the Debye peak of the Standard Anelastic Solid by a factor $r_2(\beta)$ (Nowick and Berry [11], Eq. 4.5–17), with $\beta = \sigma_P\sqrt{2}$. For $\sigma_P = 5.6$ (Table 2, specimen of experimental run 1609), and hence $\beta = 7.9$, $r_2 \sim 5$ implying $\Delta[\log(\omega\tau_P)] \sim 5.7$. The full width of the dissipation peak

Table 3

Summary of representative data for the high-temperature peak in copper in the 0.5–0.8 T_P region, for experiments where specimens were annealed above 780 °C and tested in torsional forced-oscillations, including results of the present study. T_A : annealing temperature; d : grain size (in recovered specimen); T_P : peak temperature; T_F : fusion temperature; τ_0 : limit relaxation time for the peak; E_P : peak activation energy.

Refs.	T_A , °C	d , mm	T_P , °C (at 1 Hz)	T_P/T_F	$\log_{10}(\tau_0)$, s	E_P , kJ mol ⁻¹
[20]	900	0.8	735	0.74	-23.3	435
[13]	920	0.5	~730	0.74	-21.4	444
[14]	980	0.3	780	0.78	-11.2	201
[15,41]	780	-	665	0.69	-11.9	201
[21]	?	-	600	0.64	-15.5	251
[10]	780	1	~580	~0.63	-14.9	237
[9]	820	0.8	655	0.68	-13.4	237
	1060	1.9	752	0.75	-13.4	262
	1060	4	725	0.74	-13.4	256
Exp. run 1457	1050	3–12	650	0.68	-11.5	203
Exp. run 1609	1050	1–12	645	0.68	-11.1	195

observed at fixed temperature (and hence τ_P) is thus 5.7 log units in frequency or period (broadly consistent with Figs. 4 and 5). With $\partial \ln \tau_P / \partial T = -E_P / RT^2$ (from Eq. (9)), the full width in temperature at fixed frequency or period is estimated as $\Delta T \sim (RT^2 \ln 10 / E_P) \times 5.7 \sim 350$ °C (for $T = 800$ K; cf. Fig. 8). Of course, the distribution $D_P(\ln \tau)$ of relaxation times responsible for the broad dissipation peak may reflect the superposition of multiple narrower distributions [21,17].

Comparison of the characteristics of high-temperature internal friction peak with previously available results. A comprehensive summary of torsional oscillation data for the high-temperature peak, including the results of the present study, is given in Table 3. All samples were pure polycrystalline copper annealed at temperatures greater than 780 °C — annealing conditions conducive to suppression of low to mid-temperature peak(s). Maximum strain amplitudes are all typically within the range $10^{-6} - 10^{-5}$ for all datasets (except experimental run 1457 of this study). In its general form, an Arrhenian relationship

$$\tau(T) = \tau_0 e^{E_P/(RT)} \quad (11)$$

identifies τ_0 as the “limit relaxation time”, often reported in the literature. In the extended Burgers description, values of τ_0 and peak temperature at 1 Hz are simply calculated from Eqs. (9) and (11), using fitted values of E_P and τ_{PR} .

The first notable feature in Table 3 is the absence of clear dependence of the peak temperature, or associated limit relaxation time, upon annealing temperature — and therefore upon grain size. In addition, the inferred values of E_P are consistently in the range 200–260 kJ mol⁻¹ except outliers from the pioneering studies of DeMorton and Leak [20] and Williams and Leak [13] (≈ 440 kJ mol⁻¹). Significant differences in apparent activation energy are most likely attributable to the limited period or temperature windows in the early studies.

4.4. Mechanisms responsible for anelastic relaxation in copper

The accumulation of internal friction data, on both single-crystal and polycrystalline copper, notably by Woïrgard, Rivière and co-authors, led to increasing evidence that both monotonic background damping and high-temperature internal friction peak(s) are processes resulting from *dislocation motion* controlled by diffusion (e.g., [39,19]). That both the dissipation background and peak are attributable to a common rate-controlling diffusional process is supported by evidence from this study of broadly similar activation energies obtained for

background and peak damping (Table 2). In addition, the very high levels of dispersion and dissipation for such coarse-grained materials suggest an intragranular rather than intergranular relaxation mechanism.

High-temperature internal friction peak. Mechanisms of stress relaxation at *grain boundaries* were originally invoked to explain internal friction peaks in metals, including grain-boundary sliding [22,6], grain boundary migration [5,38], twin boundary migration [20,13], and damping by dislocation jogs in grain boundaries [20,14]. As previously mentioned, the “low-temperature, grain-boundary peak” is found to markedly decline with strong grain growth upon annealing, leaving high-temperature peak(s) that remain when the grain size becomes comparable to the size of the specimen itself — as in this study for samples annealed at 1050 °C.

The inferred values of the activation energy for the high-temperature peak (Table 3) closely compare to experimental estimates for self-diffusion in copper (around 200 kJ mol⁻¹ [40]). This observation, along with low viscosities inferred from microcreep tests suggestive of linear (Harper-Dorn) dislocation creep, and the transition to non-linear behaviour most logically attributed to dislocation multiplication, are all consistent with the involvement of lattice dislocations.

5. Conclusions

We have presented the results of a broad experimental study that provides a more comprehensive assessment of the viscoelasticity of coarsely polycrystalline copper ($d \sim 3$ mm) than previously available.

For multiple specimens, annealed *in situ* at temperatures of 900 or 1050 °C approaching the melting point (1085 °C), the shear modulus G and associated strain-energy dissipation Q^{-1} were measured in forced torsional oscillation across a wide range of frequency and temperature during subsequent staged cooling.

The observed strongly viscoelastic behaviour is demonstrably independent of strain amplitude for maximum strain amplitudes $< 5 \times 10^{-6}$. However, there is clear evidence of a transition from linear to non-linear behaviour at larger strains.

Appendix: results of exploratory study for specimen annealed at 900 °C

Temporal evolution and linearity of viscoelastic behaviour

Broadly similar results were obtained during and following 27 h annealing at 900 °C, in experimental run 1390. Continuous temporal evolution was observed during annealing at 900 °C and the mechanical behaviour was found to vary significantly with stress amplitude twice and half the default value $8\tau_0$ (1000 kPa) for this experiment. Systematically higher shear modulus and lower internal friction were also found on revisiting 900 °C following staged cooling to room temperature, suggestive of limited further microstructural evolution (grain growth) during the staged cooling.

The observed dissipation involves a high-temperature background with a superimposed broad dissipation peak. Across a wide range of conditions (periods of 1–1000 s and temperatures of 350–1050 °C), the dissipation and associated modulus relaxation are described in an internally consistent manner by a model based on a Burgers creep function incorporating suitable distributions of anelastic relaxation times. Relaxation of the Young's modulus observed in parallel flexural oscillation measurements is broadly consistent with the shear modulus relaxation inferred from torsional oscillation, without requiring significant relaxation of the bulk modulus.

Similar activation energies for the relaxation times associated with the dissipation background and superimposed peak are strongly indicative of rate control by a common diffusional process. Moreover, consistency with the activation energy for lattice self-diffusion is suggestive of relaxation involving lattice dislocations in these coarse-grained copper polycrystals, in line with the findings of Woignard, Rivière and collaborators, and more recent conclusions by Benoit.

Complementary torsional microcreep data indicate that the non-elastic strain is dominantly recoverable (permanent) for loading durations $< (>) 1000$ s, thus distinguishing between the anelastic and viscous regimes. Viscosities consistently inferred from long-period torsional forced oscillation and microcreep tests are much lower than those predicted by published flow laws - suggesting a possible role for linear (Harper-Dorn) dislocation creep apparently previously unrecognised in copper, but observed in other fcc metals tested at comparably low stress amplitudes.

Acknowledgements

The experimental work described in this article was made possible by the technical support of Harri Kokkonen, Hayden Miller (ANU). The authors wish to thank Robert Rapp and Kathryn Hayward (ANU) and Pieter Vermeesch (UCL) for their participation on chemical analysis. This work was supported by grant DP130103848 from the Australian Research Council to I.J. and others.

Table A.1

Chemical analyses of the starting sample and jacket copper materials (values in weight ppm), using Ablation Inductively Coupled Plasma Mass Spectrometry (LA-ICP-MS), showing elements with resolvable concentrations (> 1 weight ppm).

	Copper sample	Copper jacket
Ag	6	5
Ni	4	3
Pb	2	5
S	60	57
Sb	1	2
Sn	1	3
Zn	1	1

Shear modulus and internal friction

Exploratory results from experimental run 1390 (Fig. A.1) are broadly consistent with those obtained on specimens annealed at 1050 °C, with a clear tendency towards higher internal friction and slightly higher shear modulus in experimental run 1390. The slopes of the $\log Q^{-1}$ vs. $\log T_0$ trends become noticeably lower towards short periods at 650 and 600 °C, and the 400 °C data defy the general trend pattern of decreasing Q^{-1} with decreasing temperature. These observations are broadly consistent with the presence of a dissipation peak superimposed upon background but the scarcity of data within the 200–600 °C interval precludes definitive interpretation.

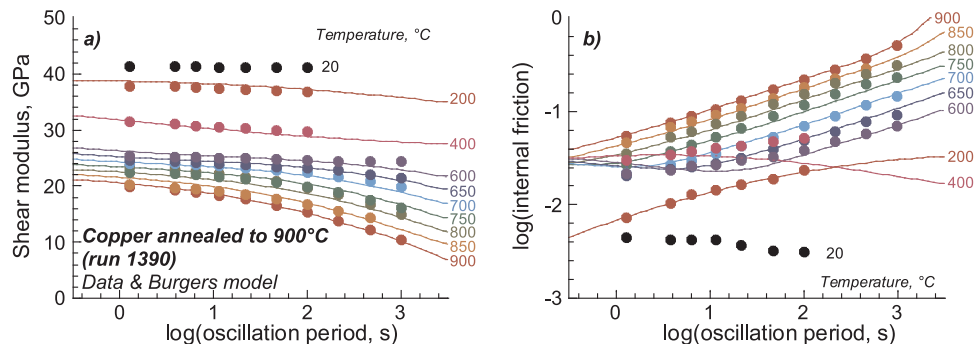


Fig. A.1. Shear modulus and internal friction (G , Q_G^{-1}) data (symbols colour-coded for temperature) for the copper specimen annealed at 900 °C during 27 h (experimental run 1390), and optimal Burgers model (colour-coded curves) fitted to $N = 83$ (G , Q_G^{-1}) data pairs (i.e., all data for temperatures between 900 and 200 °C) with misfit $\sqrt{\chi^2_{\text{tot}}/(2N)} = 0.97$. Shear stress amplitude is $8\sigma_0 = 1000$ kPa, corresponding to maximum shear strains of 45×10^{-6} , and 21×10^{-6} at 900 °C and 600 °C, respectively, at the 1000 s longest oscillation period.

Table A.2

Parameters of Andrade creep function fits to microcreep data at selected temperatures, for the copper specimen annealed at 1050 °C during 33 h (experimental run 1609). For description of parameters, see Section 2.2.3. Parameter uncertainties are parenthesised after parameter value.

T , °C	N	$J_U/10^{-2}$, $\text{rad N}^{-1} \text{m}^{-1}$	n	$\beta/10^{-4}$, $\text{rad s}^{-1/n}$ $\text{N}^{-1} \text{m}^{-1}$	$\eta_A/10^6$, Nm s rad^{-1}	$\sqrt{\chi^2/N}$
1050	4000	0.400(0.002)	0.52(0.01)	1.68(0.04)	0.1065(0.0003)	3.28
1000	4000	0.116(0.002)	0.52(0.01)	0.82(0.45)	0.282(0.002)	1.18
950	4000	0.142(0.002)	0.50(0.02)	0.52(0.05)	0.52(0.01)	0.45
900	8000	0.124(0.001)	0.51(0.01)	0.45(0.02)	1.17(0.01)	0.75
800	8000	0.136(0.002)	0.38(0.04)	0.14(0.05)	4.8(0.1)	1.03

Flexural forced-oscillation tests

The temperature-dependence of flexural forced-oscillation data was more intensively sampled on specimen 1390, in the temperature range 20–900 °C, and ranging over an additional order of magnitude in oscillation period (1–1000 s) (Fig. A.2). The normalised flexural compliance again varies systematically with temperature, and for temperature above 600 °C, also with oscillation period. The phase lag increases is about 0.005 rad for temperatures below 600 °C at all oscillation periods, and generally increases with oscillation period above 600 °C, to a maximum value near 0.02 rad at 900 °C and 1000 s oscillation period.

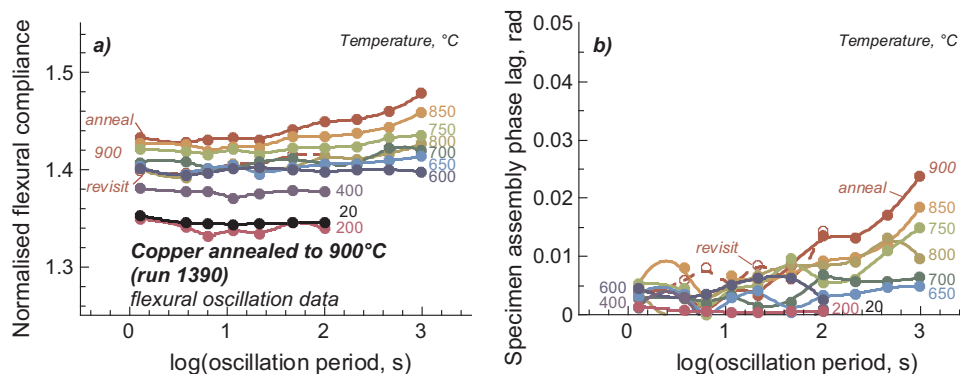


Fig. A.2. Normalised flexural compliance and phase lag data for the specimen assembly (cf. Section 2.2.2 for details) containing the copper specimen annealed at 900 °C during 27 h (experimental run 1390). At 900 °C and 101 s oscillation period, maximum flexural strain amplitude is $\sim 3 \times 10^{-6}$.

Results on the copper specimen annealed at 900 °C (Fig. A.2) are broadly similar to those obtained on the two specimens annealed at 1050 °C (Fig. 6), although a more conclusive comparison on effect of annealing temperature is limited by the differences in temperature and oscillation period sampling between specimens. The specimen annealed at 900 °C was tested at larger strain amplitudes. On that specimen, additional tests where stress amplitude was varied indicates conditions of marginally non-linear behaviour, at least at the highest temperature of 900 °C. It is therefore reasonable to assume that conditions of linear viscoelastic behaviour apply for both specimens annealed at 1050 °C.

References

- [1] T.-S. Kê, Experimental evidence of the viscous behaviour of grain boundaries in metals, *Phys. Rev.* 71 (1947) 533–546.
- [2] T.-S. Kê, Stress relaxation across grain boundaries in metals, *Phys. Rev.* 72 (1947) 41–46.
- [3] S. Weining, E. Machlin, Strain-amplitude dependent internal friction studies of dilute alloys of copper, *J. Appl. Phys.* 27 (1956) 734–738.
- [4] L. Rotherham, S. Pearson, Internal friction and grain boundary viscosity of copper and of binary copper solid solutions, *J. Metals* 8 (1956) 881–892.
- [5] G. Leak, Grain boundary damping I: pure iron, *Proc. Phys. Soc.* 78 (1961) 1520–1528.
- [6] D. Mosher, R. Raj, Use of the internal friction technique to measure rates of grain boundary sliding, *Acta Metall.* 22 (1974) 1469–1474.
- [7] J. Woïrgard, Y. Sarrazin, H. Chaumet, Apparatus for the measurement of internal friction as a function of frequency between 10^{-5} and 10 Hz, *Rev. Sci. Instrum.* 48 (1977) 1322–1325.
- [8] O. Lambri, G. Lambri, M. Torio, C. Celauro, Mechanical dynamical spectroscopy in low-flux neutron irradiated pure copper, *J. Phys.: Condens. Matter* 8 (1996) 10253–10261.
- [9] G. Ashmarin, M. Golubev, N. Naumova, A. Shalimova, *Internal Friction and Attenuation in Solids*, International Academic Publishers, Beijing, edited by T.-S. Kê, 1990.
- [10] R. Gaboriaud, J. Woïrgard, M. Gerland, A. Rivière, High-temperature isothermal internal friction of copper and copper-aluminium solid solutions between 10^{-4} and 10 Hz, *Philos. Mag. A* 43 (1981) 363–375.
- [11] A. Nowick, B. Berry, *Anelastic Relaxation in Crystalline Solids*, Academic Press, New York, 1972.
- [12] R. Schaller, G. Fantozzi, G. Gremaud, *Mechanical Spectroscopy*, Materials Science Forum, 366–368 Trans. Tech. Publications, Switzerland, 2001.
- [13] T. Williams, G. Leak, High temperature relaxation peaks in copper and aluminium, *Acta Metall.* 15 (1967) 1111–1118.
- [14] J. Roberts, P. Barrand, On the high-temperature relaxation peak in f.c.c. metals, *Metal Sci. J.* 3 (1969) 97–103.
- [15] J. Woïrgard, Résultats relatifs aux pics de frottement intérieur observés sur les métaux non alliés de structure cubique face centrée et cubique centrée au voisinage de $0,5 T_f$, *Scr. Metall.* 9 (1975) 1283–1288.
- [16] O. Lambri, A. Peñaloza, A. Morón-Alcain, M. Ortiz, F. Lucca, Mechanical dynamical spectroscopy in Cu-Li alloys produced by electrodeposition, *Mater. Sci. Eng. A* 212 (1996) 108–118.
- [17] F. Povo, B. Molinas, Present state of the controversy about the grain boundary relaxation, *Il Nuovo Cim. D* 14 (1992) 287–332.
- [18] W. Benoit, Grain boundary relaxation in metals, in: Schaller (Ed.), *Mechanical Spectroscopy*, Materials Science Forum, 366–368 Trans. Tech. Publications, Switzerland, 2001, pp. 306–314.
- [19] A. Rivière, High temperature damping, in: Schaller, et al. (Ed.), *Mechanical Spectroscopy*, Materials Science Forum, 366–368 Trans. Tech. Publications, Switzerland, 2001, pp. 268–275.
- [20] M. de Morton, G. Leak, High temperature relaxation peaks in copper and gold, *Acta Metall.* 14 (1966) 1140–1142.
- [21] A. Rivière, J. Amirault, J. Woïrgard, High temperature internal friction and dislocation motion in poly and single crystals of f.c.c. metals, *J. Phys. Colloq.* 42 (1981) 439–444.
- [22] T.-S. Kê, A grain boundary model and the mechanism of viscous intercrystalline slip, *J. Appl. Phys.* 20 (1949) 274–280.
- [23] J. Woïrgard, A. Rivière, J.D. Fouquet, Experimental and theoretical aspect of the high temperature damping of pure metals, *J. Phys. Colloq.* 42 (1981) 407–419.
- [24] W. Benoit, High-temperature relaxations, *Mater. Sci. Eng. A* 370 (2004) 12–20.
- [25] A. Rivière, Low frequency techniques, in: Schaller, et al. (Ed.), *Mechanical Spectroscopy*, Materials Science Forum, 366–368 Trans. Tech. Publications, Switzerland, 2001, pp. 635–651.
- [26] J. Minster, D. Anderson, A model of dislocation-controlled rheology for the mantle, *Philos. Trans. R. Soc. Lond.* 299 (1981) 319–356.
- [27] G. Schoeck, E. Bisogni, J. Shyne, The activation energy of high temperature internal friction, *Acta Metall.* 12 (1964) 1466–1468.
- [28] I. Jackson, U. Faul, R. Skelton, Elastically accommodated grain-boundary sliding: new insights from experiment and modeling, *Phys. Earth Planet. Inter.* 228 (2014) 203–210.
- [29] I. Jackson, M. Paterson, A high-pressure, high-temperature apparatus for studies of seismic wave dispersion and attenuation, *Pure Appl. Geophys.* 141 (1993) 445–466.
- [30] C. Cline, I. Jackson, Relaxation of the bulk modulus in partially molten dunite? *Geophys. Res. Lett.* 43 (2016) 11644–11651.
- [31] I. Jackson, A. Barnhoorn, Y. Aizawa, C. Saint, Improved procedures for the laboratory study of high-temperature viscoelastic relaxation, *Phys. Earth Planet. Inter.* 172 (2009) 104–115.
- [32] I. Jackson, J. Fitzgerald, H. Kokkonen, High-temperature viscoelastic relaxation in iron and its implications for the shear modulus and attenuation of the earth's inner core, *J. Geophys. Res.* 105 (2000) 23605–23634.
- [33] I. Jackson, H. Schijns, D. Schmitt, J. Mu, A. Delmenico, A versatile facility for laboratory studies of viscoelastic and poroelastic behaviour of rocks, *Rev. Sci. Instrum.* 82 (2011) 064501.
- [34] A. Barnhoorn, I. Jackson, J. Fitzgerald, A. Kishimoto, K. Itatani, Grain size-sensitive viscoelastic relaxation and seismic properties of polycrystalline MgO, *J. Geophys. Res.* 121 (2016) 4955–4976.
- [35] I. Jackson, U. Faul, Grain-size-sensitive viscoelastic relaxation in olivine: towards a robust laboratory-based model for seismological application, *Phys. Earth Planet. Inter.* 183 (2010) 151–163.
- [36] A. Nowick, Internal friction and dynamic modulus of cold-worked metals, *J. Appl. Phys.* 25 (1954) 1129–1134.
- [37] H. Frost, M. Ashby, *Deformation-Mechanism Maps. The Plasticity and Creep of Metals and Ceramics*, Pergamon, Tarrytown, N.Y., 1982.
- [38] M. de Morton, G. Leak, Grain-boundary relaxation in Cu-Au alloys, *Metal. Sci. J.* 1 (1967) 166–170.
- [39] M. Nô, C. Esnouf, J.S. Juan, G. Fantozzi, Internal friction at medium temperature in high purity aluminium and its relation with the microstructure - II, *Acta Metall.* 36 (1988) 837–845.
- [40] K. Maier, Self-diffusion in copper at low temperatures, *Phys. Status Solidi (a)* 44 (1977) 567–576.
- [41] J. Woïrgard, Modèle pour les pics de frottement interne observés à haute température sur les monocristaux, *Philos. Mag.* 33 (1976) 623–637.